Effect of Areal Chain Density on the Location of Polymer-Modified Gold Nanoparticles in a Block Copolymer Template

Bumjoon J. Kim,[†,‡] Joona Bang,[‡,#] Craig J. Hawker[⊥,‡,§] and Edward J. Kramer*,[†,‡,§]

Department of Chemical Engineering, Materials Research Laboratory, Department of Materials, and Department of Chemistry, University of California, Santa Barbara, Santa Barbara, California 93106, and Department of Chemical and Biological Engineering, Korea University, Seoul 136-701, Republic of Korea

Received February 9, 2006; Revised Manuscript Received April 4, 2006

ABSTRACT: A strategy for controlling the location of gold nanoparticles within block copolymer domains through varying the surface coverage of gold nanoparticles by end-attached polymer ligands is described. Gold nanoparticles coated by short thiol end functional polystyrene homopolymers (PS-SH) (M_n = 3.4 kg/mol) are incorporated into a poly(styrene-*b*-2-vinylpyridine) diblock copolymer template (PS-*b*-P2VP) (M_n = 196 kg/mol), the P2VP block of which has a more favorable interaction with a bare gold particle surface than does the PS block. The areal chain density of the PS-SH ligands on gold particles is varied by changing the mole ratio of PS-SH chains to gold atoms. It is found that the areal density of PS chains on the gold particles is critical to controlling their location in block copolymer templates. PS-coated gold nanoparticles with PS chain areal density higher than 1.6 chains/nm^2 are dispersed in PS domains of PS-*b*-P2VP while they are segregated along the interface between PS and P2VP domains of PS-*b*-P2VP for PS chain areal density <1.3 chains/nm^2. Even at extremely low grafting densities of polymer ligands, gold nanoparticles can be stabilized in solution, and self-assembly of these nanoparticles can be controlled within the block copolymer template.

Introduction

Incorporation of nanoparticles into block copolymers has been explored as an efficient way for the fabrication of novel functional materials such as nanostructured solar cells, photonic band-gap materials, highly efficient catalysts, and high-density magnetic storage media. Several experimental methods have been developed for incorporating inorganic nanoparticles into polymeric nanostructures.[1−14] The most popular approach involves the synthesis of nanoparticles in situ within the block copolymer template by using preformed micelles of block copolymers containing metal precursors. However, despite the importance of controlling the arrangement of nanoparticles produced by such methods within the periodic structure of the block copolymer, establishing such control has been difficult. Another approach, recently proposed as a possible way to overcome some of these drawbacks, uses cooperative self-organization of preformed nanoparticles and block copolymers. On the basis of theoretical predictions for inorganic−organic nanocomposties by Balazs and co-workers,[15−17] Bockstaller et al.[1,2] demonstrated hierarchical pattern formation of silica and gold nanoparticles coated by short organic molecules using binary mixtures of nanoparticles and block copolymers. More recently, Chiu et al.[3] showed that the nanoparticle location within an A−B block copolymer templates coated by a mixture of end-functional A and B homopolymers to the nanoparticle surface can be controlled by exploiting the enthalpic interaction between the block copolymer and the polymer-coated nanoparticles. However, this strategy requires the synthesis of two different polymer ligands, one matching each of the block copolymer

domains, which are used as mixtures during synthesis of the Au nanoparticles.

An important role of these polymeric ligands is to stabilize and control nanoparticle formation during solution synthesis, allowing the initial small size to be maintained by preventing coagulation. At the same time, by specifying the chemical nature so that they interact more favorably with the A block and the B block or provide a "neutral" polymer surface to the nanoparticle, these ligands can provide an ability to accurately control the placement of nanoparticles within the block copolymer template.[2,3] Therefore, an understanding of the interaction between the particle surface, ligands on the surface, and the polymer matrix is critical for developing standard rules for controlling the 3-dimensional structure of particle−organic hybrid nanomaterials. This is a grand challenge, however, since the pairwise interactions between different species are very complex and are difficult to predict *a priori*. For example, it is unclear how many ligands per unit area on the nanoparticle surface are required to shield the particle surface from the polymer matrix. To begin to address this grand challenge, a systematic investigation of the effect of surface coverage was initiated using a model system with the following characteristics. First, nanoparticles that permit a wide range of areal chain densities to be assembled on their surfaces are required. Small (2−5 nm diameter) gold nanoparticles satisfy the requirement as the high surface area coupled with efficient reaction with thiol end-functional short chain leads to the assembling of such chains on the particle surface by the "grafting-to" method.[18,19] Second, the use of a block copolymer template that has one block that is known to interact with the gold nanoparticles more favorably than the other block is essential. For gold nanoparticles, such information can be obtained from the ordering of symmetric A−B diblock copolymers on a flat gold-coated surface, where favorable interaction will lead to segregation of one block to the Au surface. This segregation can be determined by dynamic secondary mass spectrometry or by neutron

† Department of Chemical Engineering, UC, Santa Barbara.
‡ Materials Research Laboratory, UC, Santa Barbara.
§ Department of Materials, UC, Santa Barbara.
⊥ Department of Chemistry, UC, Santa Barbara.
Korea University.
* Corresponding author: e-mail edkramer@mrl.ucsb.edu.

Table 1. Characterization of Gold Nanoparticle Coated by PS Chains (M_n = 3.4 kg/mol) Synthesized with Various Initial Mole Ratio of PS Chains to (Gold Atoms plus PS Chains) (f_{PS})

f_{PS}[a]	weight ratio of polymer to gold[b]	⟨particle core diameter⟩ (nm)[c]	⟨particle diameter⟩ (core + shell) (nm)	areal chain density Σ (chains/nm²)
0.2	1.42	2.05	6.14	1.64
0.143	1.08	2.56	7.04	1.57
0.125	1	2.54	6.82	1.45
0.11	0.81	2.584	6.49	1.19
0.1	0.79	2.71	6.75	1.22
0.091	0.733	2.68	6.74	1.12
0.077	0.528	2.76	6.08	0.83
0.059	0.55	2.82	6.29	0.88
0.0476	0.422	2.74	5.65	0.66
0.04	0.38	3.46	6.91	0.75
0.033	0.24	3.31	5.81	0.45
0.0154	0.11	5.11	7.39	0.32
0.0077	0.0723			

[a] f_{PS} = initial mole ratio of PS ligands to (Au atoms plus PS ligands) in particle synthesis. [b] Measured by TGA. [c] Obtained from image analysis based on TEM images for at least 300 particles.

reflectometry of deuterium-labeled block copolymers and is known for a number of A−B diblock copolymers.[20]

In this paper, we demonstrate a simple procedure to control the location of polymer-coated gold nanoparticles within A−B block copolymer domains by variation of a single parameter, the surface coverage of gold nanoparticles by a homopolymer A ligand. As the areal density of A chains on the nanoparticle decreases, a sharp transition from the case where the particles are located in the A domain to the case where particles are located at the A−B interface is observed and is driven by the favorable interaction of the B block with the nanoparticles. Based on the areal density for this transition, an understanding of the chain structure of the A shell of the nanoparticle required to prevent the interaction between the Au surface and the B block is developed.

Experimental Section

Synthesis of Thiol-Terminated PS and P2VP. A symmetric poly(styrene-*b*-2-vinylpyridine) (PS-*b*-P2VP) diblock copolymer with total molecular weight $M_n \sim$ 196 500 g/mol and a polydispersity (PDI) of 1.11 (Polymer Source, Inc.) was used as the block copolymer template in which to investigate the position of gold nanoparticles systematically. To incorporate gold nanoparticles into PS-*b*-P2VP block copolymer template, those particles are stabilized by thiol-terminated PS (PS-SH). PS-SH was synthesized by living anionic polymerization using benzene as solvent at 30 °C.[5] Polymerization of styrene was initiated by *sec*-butyllithium and allowed to proceed for 3 h under nitrogen. Polystyryl anions were then titrated by ethylene sulfide, after which the sulfide ends were protonated by acidic methanol. The molecular mass M_n and polydispersity index of PS-SH was 3.4 kg/mol and 1.15, respectively. Thiol-terminated P2VP with a M_n of 3 kg/mol and a PDI of 1.10 was synthesized by living anionic polymerization following the same procedure described for the synthesis of PS-SH.

Synthesis of PS- and P2VP-Coated Au Nanoparticles. The synthesis of PS-coated Au nanoparticles synthesis was accomplished using a two-phase system[21] consisting of toluene and water by varying the initial mole feed ratio of PS ligands to (Au atoms + PS ligands) from 1/5 (=0.2) to 1/129 (=0.0077). The characteristics of these polymer-coated gold nanoparticles are summarized in Table 1. The polymer-coated gold particles were separated from unattached PS thiol by precipitation using a mixture of ethanol and toluene, concentrating the particles by centrifugation followed by membrane filtration (MWCO 30 000 Da, Millipore, Inc.) using dimethylformamide (DMF) as a solvent. Finally, those particles were redispersed in dioxane and washed by membrane filtration

twice and subsequently washed with methanol to remove ungrafted ligands as well as any residual reducing agent.

As P2VP is not soluble in toluene, an alternative, one-phase method using dry THF was employed to synthesize P2VP-coated Au nanoparticles. Initially, gold precursors (HAuCl₄) and P2VP ligands with various f_{P2VP} ratios were dissolved into dry THF and mixed for 15 min under a nitrogen atmosphere. Gold particles were synthesized by adding a reducing agent, superhydride (1.0 M Li-(C₂H₅)₃BH in THF from Sigma-Aldrich), dropwise under nitrogen.[22] The addition of the reducing agent was continued dropwise until no more gas was evolved. Particles were purified by membrane filtration using DMF, dioxane, and methanol sequentially to remove ungrafted ligands as well as residual reducing agent as described for the PS−Au particles. Several different P2VP-coated Au particles were synthesized with various initial molar ratios of P2VP ligands to (Au atoms + P2VP ligands) (f_{P2VP}) from 2 to 0.015.

Preparation of PS-*b*-P2VP/Polymer-Coated Au Nanoparticle Composites. To prepare the nanocomposite samples, a 1 wt % block copolymer solution in dichloromethane was mixed with PS-coated gold nanoparticles (PS−Au) to produce a weight fraction of ∼0.15. A particle/block copolymer composite was prepared by solvent casting a mixture of PS−Au nanoparticles and PS-*b*-P2VP block copolymer in dichloromethane onto an epoxy substrate and then annealing under a saturated solvent atmosphere at 25 °C for at least a day. All solvent in the sample was forced to evaporate very slowly over an additional day. Samples were subsequently dried in the air overnight and further under vacuum for 4 h to make sure that no solvent is left in the sample. As a result, a 10−20 μm thick film of nanoparticle/block copolymer composite was produced.

Characterization. The size of the polymer-coated gold nanoparticle and the location of the PS-coated gold particles (PS−Au) and the P2VP-coated gold particles (P2VP−Au) in the PS-*b*-P2VP were determined by transmission electron microscopy (TEM) using a FEI Tecnai G2 microscope operated at 200 kV. Gold nanoparticles coated by PS chains were dissolved at a very low concentration in dichloromethane or THF. A 20−30 nm thick carbon film-coated TEM grid was dipped into the solution for a second, dried in the air, and then examined by TEM. Samples of gold nanoparticle−block copolymer composites were prepared for cross-sectional TEM by microtoming epoxy-supported thick films into 25−40 nm slices that were then stained by exposing them to iodine vapor, which selectively stains the P2VP domains.

The gold core diameter distribution obtained as a histogram from TEM image analysis was used to calculate the average surface area per gold nanoparticle. Weight fractions of gold and polymer ligands were measured by thermal gravimetric analysis (TGA). These numbers were confirmed by elemental analysis. The weight fraction of carbon, hydrogen, and nitrogen in polymer-coated Au particles was measured, and the weight fraction of residue was assumed to be that of the gold core. The weight fractions of the polymer chains were converted into volume fractions using the density of the polymer (∼1.05 g/cm³) and the density of the gold particles (∼19.3 g/cm³). The number of polymer ligands per each gold particle for various core−shell type particles, divided by the average surface area of the gold particle, gives the chain areal density of polymer ligands on the particle surface.

Results and Discussion

The nanoparticle Au core diameter is shown as a function of initial mole ratio of PS ligands to gold atoms in Figure 1. The average particle core (Au) diameter for each mole ratio was determined from TEM images by analyzing at least 300 particles using standard image analysis software (Image Pro). The error bars in Figure 1 represent the standard deviation of the particle diameter. The particle core diameter for each set of gold particles is also listed in Table 1. The particle core diameter is found to depend on initial mole feed ratio of PS ligands to (Au atoms + PS ligands) (f_{PS}). It increases from 2.1 ± 0.7 to 2.8 ± 1.0 nm as f_{PS} decreases from 0.2 to 0.059. As f_{PS} decreases, the particles
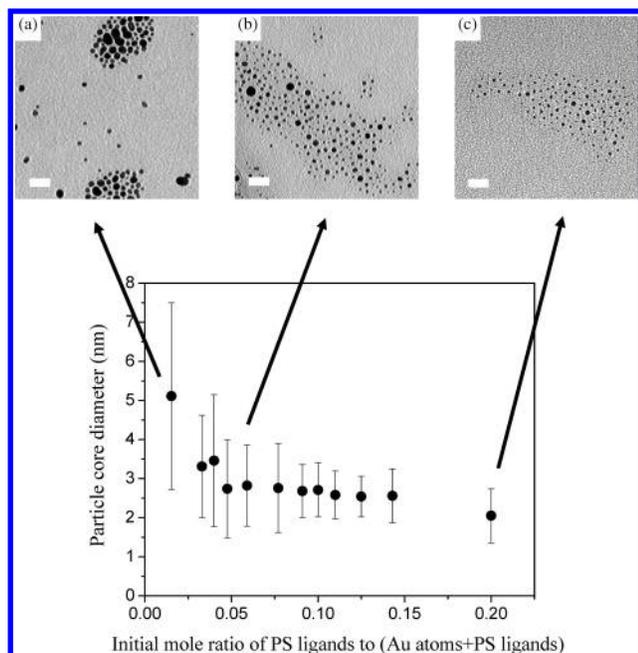
Figure 1. Particle Au core size is shown as a function of initial mole ratio of PS ligands to (Au atoms + PS ligands) (f_{PS}) during synthesis. These numbers are obtained from image analysis of TEM images at least 300 particles for each f_{PS} value. Error bars represent the stardard deviation of the particle diameter. As f_{PS} is decreased, the particles are getting larger and more polydisperse. Three TEM images of (a), (b), and (c) represent particles for f_{PS} = 0.015, 0.059, and 0.2, respectively. (a) Particle core diameter = 2.05 ± 0.69 nm, (b) 2.82 ± 1.04 nm, and (c) 5.11 ± 2.39 nm. Scale bar is 20 nm.

also become more polydisperse in size, as shown in the TEM images of Figure 1a−c, which represent particles with a particle core diameter = (a) 2.05 ± 0.69 nm, (b) 2.82 ± 1.04 nm, and (c) 5.11 ± 2.39 nm for f_{PS} = 0.2, 0.059, and 0.015, respectively. This trend is consistent with the results observed by Shimmin et al.[23] for poly(ethylene glycol)-coated gold particles and Leff et al.[24] and Hostetler et al.[25] for dodecane-coated gold particles. In toluene solution, the gold particles were observed to be stable even at extremely low f_{PS} such as 0.0077, despite their increased size and polydispersity. These particles are stable even after several washing cycles. After the f_{PS} = 0.0077 synthesis and incorporation of the gold nanoparticles into the block copolymer template, individual PS−Au particles are observed by TEM to be reasonably well dispersed without serious aggregation. Grafting densities of polymer ligands on the particle surface for various core−shell type particles were estimated on the basis of weight fractions of gold and polymer ligands obtained from elemental analysis and TGA to determine the core−shell structure including polymer shell thickness and PS chain areal density on gold particle surface. The estimated mean particle diameter including both the Au core and the polymer shell is shown in Figure 2 for various f_{PS} values. Since the weight fraction of polymer ligands in polymer-coated particles decreases as f_{PS} decreases, the PS shell thickness becomes smaller. A dotted line in Figure 2 indicates the f_{PS} value where the polymer shell thickness is equivalent to the radius of gyration (R_g) of the polymer ligands grafted on the particle surface.

   The cross-sectional TEM images of Figure 3 show PS-coated particles with different PS grafting densities on their surface dispersed in the PS-*b*-P2VP lamellar diblock copolymer. Since the P2VP domain is selectively stained by iodine vapor, the darker domain in the images corresponds to the P2VP domain. From Figure 3 it is clear that the particles are located near the center of the PS domains (lighter regions) when the PS grafting
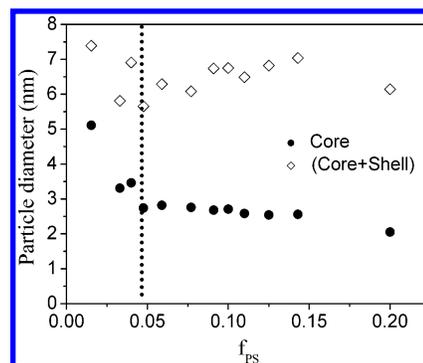

Figure 2. Particle core diameter and polymer shell thickness for various f_{PS} values are shown in the graph. The PS shell thickness on gold surface and the volume fraction of the PS shell are estimated on the basis of weight fractions of gold and polymer ligands obtained from elemental analysis and thermal gravimetric analysis. Since the weight fraction of polymer ligands decreases as f_{PS} decreases, the PS shell thickness becomes smaller. A dotted line represents the f_{PS} value where the polymer shell thickness is same as the radius of gyration, R_g, of polymer ligand.
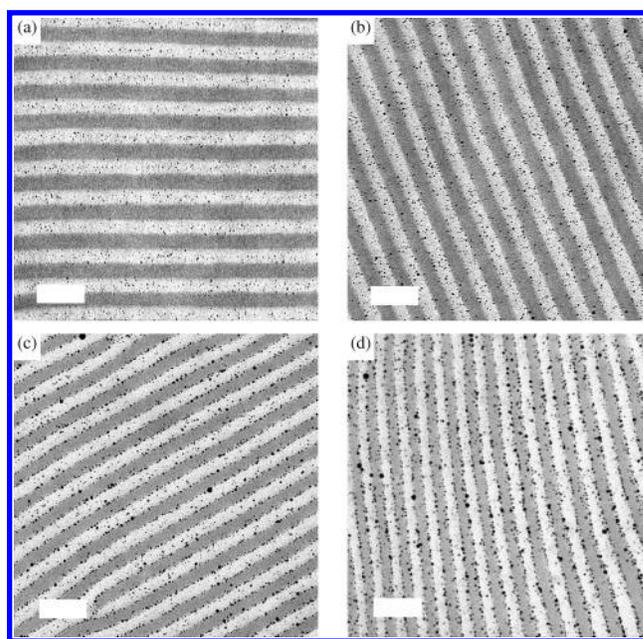

Figure 3. Cross-sectional TEM images of PS-*b*-P2VP block copolymer containing PS-coated gold nanoparticles whose surfaces are covered with various chain areal densities of PS chains (M_n = 3.4 kg/mol): (a) 1.64, (b) 1.45, (c) 1.22, and (d) 0.83 chains/nm². Scale bar is 100 nm.

density is relatively high as in (a) 1.64 chains/nm². As the particle grafting density decreases, particles are distributed roughly equally between the center of the domain and the interfaces as seen in Figure 3b, corresponding to 1.45 chains/nm². As the PS grafting density on the gold surface decreases further from 1.45 to 1.22 chains/nm² (Figure 3c), most nanoparticles are clearly segregated along the interface between PS and P2VP, and at a PS grafting density of 0.83 chains/nm² virtually all nanoparticles are at the PS/P2VP interface. Histograms of the particle locations for these samples are shown in Figure 4 and serve to quantitatively reinforce the qualitative impressions from examining the TEM micrographs. To illustrate the effect of variations in the PS grafting density on controlling the self-assembly of nanoparticles in the block copolymer template, the PS chain areal density on the particle surface is shown as a function of f_{PS} in Figure 5. The PS chain areal density on the nanoparticle surface increases from 0.66 to 1.64 chains/nm² as f_{PS} increases from 0.045 to 0.2. We did not observe a
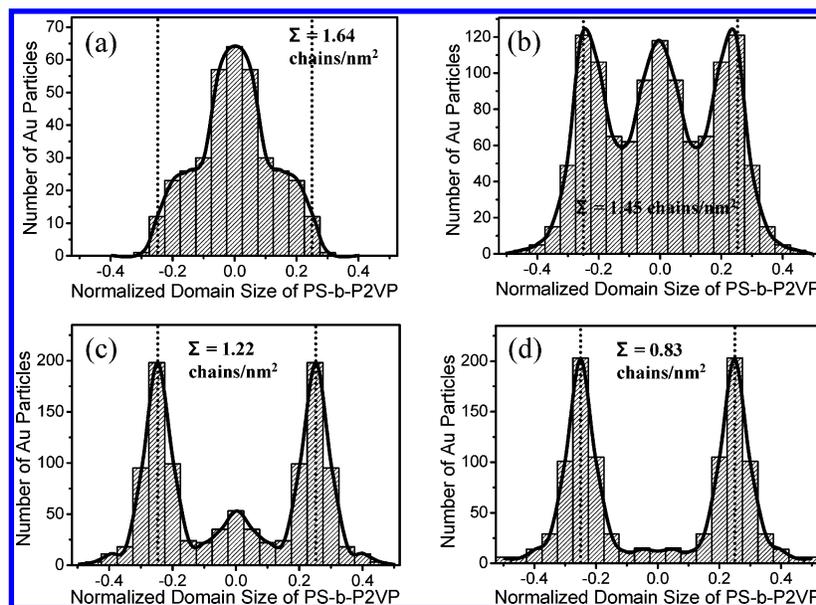
Figure 4. Histograms of particle positions from the TEM micrographs in Figure 3: (a) 1.64, (b) 1.45, (c) 1.22, and (d) 0.83 chains/nm^2. Interfaces of the PS domain are at -0.25 and $+0.25$, and data are averaged at a given position relative to zero, i.e., number of particles at $-0.2 =$ (number of particles at $-0.2 +$ number of particles at $+0.2$)/2.
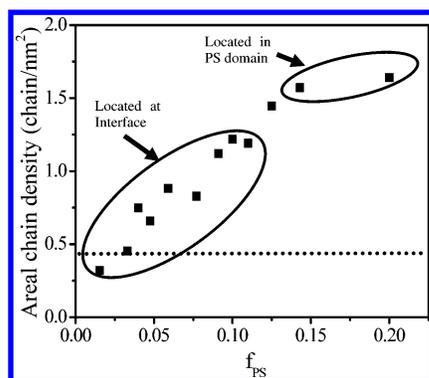

Figure 5. Effect of PS grafting densities on particle location in the PS-*b*-PVP block copolymer template. The PS grafting density can be varied by initial mole feed ratio of PS to Au atoms during synthesis as shown in the graph. For points above 1.5 chains/nm^2 the PS$-$Au particles are located in the PS domain of the block copolymer, whereas for points below 1.3 chains/nm^2 the PS$-$Au particles are located at the PS-*b*-P2VP interface. The transition areal density ($\sim$1.4 chains/ nm^2) is much higher than $1/R_g^2$, which is indicated by the dotted line in the graph.

significant increase in Au particle size until f_{PS} is less than 0.03, corresponding to a chain areal density of 0.45 chains/nm^2. The PS chain areal density is strongly dependent on f_{PS} in this low-f_{PS} regime. However, it should be noted that the PS area chain density on the Au surface approaches saturation when the initial mole feed ratio f_{PS} of PS to (Au + PS) is larger than 0.5. As shown in Figure 3, the change of PS grafting density induces a transition of nanoparticle location from the PS domain to the PS-*b*-P2VP interface. Two different regimes can be identified in Figure 4 and show how the nanoparticle position in the block copolymer templates depends on the areal density of PS chains. When the chain areal density is higher than 1.5 chains/nm^2, nanoparticles are clearly dispersed near the center of the PS domains. This localization of nanoparticles coated with polymer A near the center of the A polymer domain in a A$-$B diblock copolymer system is consistent with recent simulations.[15$-$17]

Of particular interest, however, is the observation of a transition in the nanoparticle location induced by a decrease in PS chain areal density from 1.6 to 1.2 chains/nm^2. Our rationale
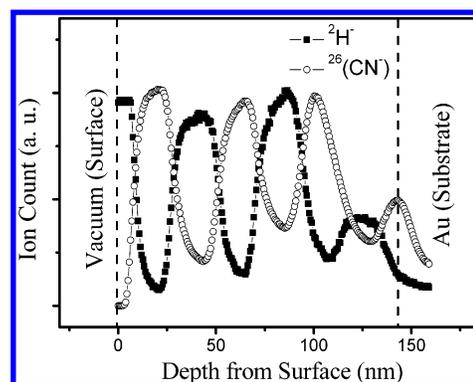

Figure 6. Dynamic SIMS depth profiles of ^{2}H$^-$ and CN$^-$ signals from the dPS and P2VP domains, respectively, of a lamellar dPS-*b*-P2VP block copolymer film on a 300 nm thick Au film showing that the P2VP domain preferentially segregates to the block copolymer/Au interface.

for this behavior is that nanoparticles with PS chain areal densities <1.3 chains/nm^2 do not fully shield the Au nanoparticle surface from interacting with the P2VP block of the PS-*b*-P2VP matrix. There is a favorable interaction between gold and P2VP while the PS/gold interaction is relatively weaker.[26]

To directly demonstrate that such a favorable interaction exists, we have spin-cast a 115 nm thick film of dPS-*b*-P2VP from a solution in toluene on a 300 nm thick Au film that was deposited on a 20 nm thick Ti film on a silicon substrate. The dPS and P2VP blocks of the dPS-*b*-P2VP copolymer synthesized by living anionic polymerization at UCSB have number-average molecular weights of 32 and 28 kg/mol. The block copolymer film was annealed at 180 °C for 40 h to obtain an equilibrium layered structure on the Au surface. By optical microscopy and scanning force microscopy the annealed film had islands on its surface $\sim$40 nm high. The depth profile of ^{2}H$^-$ and ^{26}(CN$^-$) ions from the dPS and P2VP, respectively, in the film was determined by dynamic secondary ion mass spectrometry (DSIMS) using a Physical Electronics 6650 instrument. Negative ions were detected as polymer is sputtered by an incident beam of 1 keV O$_2^+$ ions. Figure 6 shows clearly the layered structure of the lamellar dPS-*b*-P2VP block copolymer consisting of a

surface half lamella of dPS on the surface and a half lamella of P2VP on the Au substrate. (The decreased yield of $^2H^-$ and $^{26}(CN^-)$ ions from the deepest set of dPS and P2VP layers is due to the fact that this signal comes from the island regions of the film.)

Further evidence for a strong P2VP interaction with Au comes from the experiments of Kunz et al.,[26] who showed that P2VP has a very low contact angle with Au (9°) and that 20 nm diameter Au nanoparticles (initially stabilized by citrate ions in solution) placed at a PS−P2VP interface diffuse into the P2VP when the interface is annealed at the temperature above 100 °C. Gittins et al.[27] and Gandribert et al.[28] stabilized gold particles by 4-(dimethylamino)pyridine using the favorable interaction between pyridine and gold particle surface.

In our experiments, we also observed the consequences of a relatively stronger interaction of P2VP with the Au surface during the synthesis of the Au nanoparticles. When P2VP-SH ligands of comparable molecular weight to the PS-SH ligands were used, the areal density of P2VP thiol chains on the Au nanoparticle surface was significantly lower than that of PS thiol chains at the same initial mole ratio of polymer ligands to (gold atoms + polymer ligands) ($f_{PS} = 0.2$). For example, at an $f_{PS} = 0.2$ where the areal density of PS-SH chains on the Au particle surface is 1.64 chains/nm^2, the areal density of P2VP-SH chains on P2VP-coated particles synthesized with $f_{P2VP} = 0.2$ is 1.13 chains/nm^2. The relatively strong interaction of P2VP with the Au particle surface apparently competes with that of the thiol end group, leading to a larger molecular foot print.

For the sample with $\Sigma = 1.45$ chains/nm^2 there are approximately equal numbers of particles at the interface as in the center of the PS domain, as seen in Figure 4. Histograms that attempt to distinguish small from large particles lead to similar results. We suspect, but cannot prove, that the reason for the different behavior of different particles is the fact that the average number $\langle n \rangle$ of PS-SH chains bound to the very small Au particles is quite small. For example in the $\Sigma = 1.45$ chains/nm^2 sample $\langle n \rangle = 31$. If the numbers of PS-SH chains per particle are normally distributed, that implies a standard deviation for n of 5.7 chains, and thus a significant fraction of particles will have more than 37 chains ($\Sigma = 1.76$ chains/nm^2) and less than 25 ($\Sigma = 1.19$ chains/nm^2). Thus, intermediate segregation behavior as observed for an average grafting density of 1.45 chains/nm^2 is to be expected.

To confirm that the favorable interaction of the gold surface with the P2VP domain of PS-*b*-P2VP is responsible for inducing particles with PS areal chain densities less than 1.3 chains/nm^2 to segregate to the interface of block copolymer template, a control experiment was performed. Several different P2VP-coated Au particles were synthesized with various initial molar ratios of P2VP-SH ligands ($M_n = 3$ kg/mol, PDI = 1.10) to Au atoms (f_{P2VP}) from 2 to 0.015. Nanoparticles synthesized with a low f_{P2VP} such as 0.03 and 0.015 appear stable just after synthesis but aggregate during the washing procedure so that only large aggregates are observed in the TEM images. In contrast, gold nanoparticles with $f_{P2VP} > 0.03$ synthesized by the one-phase method are stable to washing. These stable P2VP-coated Au (P2VP−Au) particles were then mixed with the PS-*b*-P2VP block copolymer in a dichloromethane solution and solvent cast as described for the PS−Au and PS-*b*-P2VP nanocomposites. All P2VP-coated particles synthesized at higher f_{P2VP} values are observed to be dispersed inside the P2VP domains of the PS-*b*-P2VP template regardless of the areal chain densities of P2VP ligands. Two different TEM images of the P2VP-coated gold nanoparticles synthesized with f_{P2VP} of 0.2
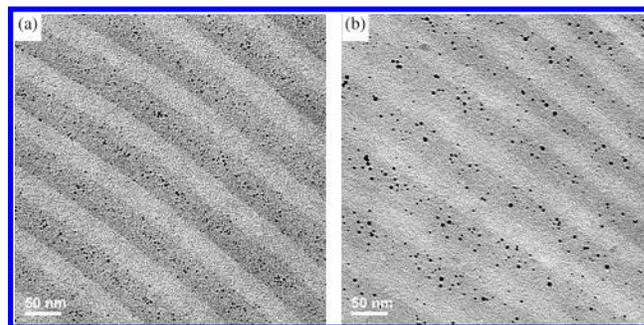

Figure 7. Cross-sectional TEM image of P2VP-coated gold nanoparticles in PS-*b*-P2VP. Initial mole ratios of P2VP ligands to (Au atoms + P2VP ligands) for (a) and (b) are 0.2 and 0.059, respectively. P2VP-coated Au particles are dispersed in the P2VP domain of PS-*b*-P2VP even at low chain areal densities of (a) 1.14 and (b) 0.76 chains/nm^2.

and 0.059 in the PS-*b*-P2VP template are shown in parts a and b of Figure 7, respectively. Like PS-coated gold nanoparticles, as f_{PVP} decreases from 0.2 to 0.059, particle size increases as can be seen by comparing parts a and b in Figure 7. While Au nanoparticles with large f_{P2VP} ($f_{P2VP} = 2$ at areal chain density = 2.36 chains/nm^2) are found in the P2VP domain in analogy to what we observe for the high areal chain density PS−Au nanoparticles that segregate to the PS domain, the P2VP-coated Au particles with low chain areal densities of 1.14 chains/nm^2 (Figure 7a) and 0.76 chains/nm^2 (Figure 7b) are also clearly dispersed in the P2VP domains of PS-*b*-P2VP rather than segregated to the PS-*b*-P2VP interface, in clear contrast to the low areal chain density PS−Au particles. These low areal chain density PS−Au nanoparticles thus segregate to the interface due to the inability of the low-density PS brush to screen the favorable interaction between the P2VP block chains and the bare Au surface.

As shown in Figures 3−5, the areal chain density of PS ligands is critical for controlling the nanoparticle location within the PS-*b*-P2VP template. Only f_{PS} was varied to control the areal density in that experiment. However, the f_{PS} ratio also has an effect on the particle size. Though this effect is very small in the regime where the transition of nanoparticle position occurs, it is observed that the nanoparticle size does increase slightly as the f_{PS} used for the particle synthesis decreases. Since the adsorption energy of particles at an A−B interface can be expressed as $E_a = \pi r^2 \gamma_{AB}(1 - |\cos \theta|)^2$, where r is the radius of the nanoparticle, $\cos \theta$ is the contact angle of the nanoparticle at the interface between A and B layers, and γ_{AB} is the interfacial tension between A and B layers,[29] larger particles will have a higher adsorption energy, which means that the larger particles produced using small f_{PS} can be adsorbed at the interface more favorably. To isolate the areal chain density influence from the particle size effect on the particle location and confirm that the chain areal density effect has a major influence on the particle location, the following experiment was performed. Two different gold particles were synthesized with similar initial f_{PS} during synthesis but by different synthesis methods ((a) the one-phase method (THF) and (b) the two-phase method (water/toluene)). Initial molar ratios ($f_{PS} = 0.11$ and $f_{PS} = 0.10$) of PS ligands to (gold atoms + PS ligands) (f_{PS}) were used for the one-phase method synthesis and two-phase method synthesis, respectively. These two different synthetic methods give nanoparticles with the same value for the weight ratio of PS chains to Au (0.8 for both particles shown in Figure 8a,b). However, they produce nanoparticles with different Au core diameters and therefore different areal chain densities of the PS chains on the Au nanoparticle. The average nanoparticle core diameter for the
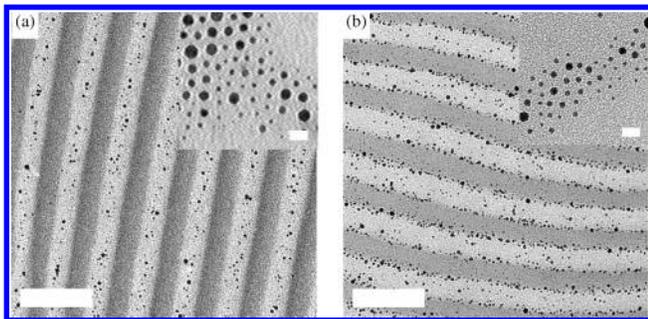
Figure 8. Effect of PS grafting densities on particle location in PS-*b*-PVP block copolymer template. Two different gold particles are synthesized using similar f_{PS} values ((a) 0.11, (b) 0.10) but by different synthesis methods ((a) one-phase method using THF; (b) two-phase method (water/toluene)). The different synthesis methods give same value for the weight ratio of PS chains to Au (0.8 for both particles shown in (a) and (b)), but different particle core diameters as shown in the TEM image of the small window in the right-hand corner. The PS grafting density for particles in (a) is 1.7 chains/nm^2 while that in (b) is only 1.2 chains/nm^2. Particles in (a) are dispersed only in the PS domain while those in (b) are located mainly at the PS-*b*-P2VP interface. Scale bar is 100 nm in the main image and 10 nm in the small window.

one phase method is 3.7 nm while that for the two-phase method is 2.7 nm as shown in the small TEM image inset in Figure 8a,b, and this leads to an areal chain density for the PS−Au nanoparticles in Figure 8a of 1.7 chains/nm^2, which is slightly higher than 1.4 chains/nm^2, the value from Figure 5 corresponding to the transition from the middle of PS domain to being located at the PS-*b*-P2VP interface. In contrast, the density for the nanoparticles in Figure 8b is only 1.2 chains/nm^2, well below 1.4 chains/nm^2. Clearly, nanoparticles in Figure 8a are dispersed only in the PS domain while those in Figure 8b are located mainly at the interface. This result implies that nanoparticle size is not as important as areal chain density for deciding the particle position.

The experiments described above demonstrate that this ability to precisely control nanoparticle location within a block copolymer matrix relies on the enthalpic interactions between the particle surface, the polymer ligands on the surface, and the block copolymer template, interactions that depend on the chain areal density of polymer ligands. To further investigate the critical nature of polymer chain formation in these systems, the extent of PS coverage of the surface or how much stretching of the PS chains is required to shield the interaction between PVP matrix and the surface of gold particle was studied. To quantify the amount of PS ligands on the Au particle surface, a standard method for calculating the chain areal density was used.[1,3,19] The ability of the PS chain ligands to shield the surface of the gold nanoparticles from the P2VP block chains logically depend on the character of the PS brush assembled on the gold nanoparticle. If this brush is stretched, an entropic barrier must be overcome for P2VP to reach the gold surface, in addition to the unfavorable enthalpy of interaction between PS and P2VP. One possible criterion for the onset of stretching is when the area per chain on the surface of gold particle is less than R_g^2, where R_g is the radius of gyration of the PS ligand. The corresponding areal chain density $(1/R_g^2)$ is 0.41 nm^{-2} (dotted line in Figure 5), considerably below the value of 1.45 chains/nm^2, where the transition in particle position is observed.

The gold particle surface is highly curved, however, while the single chain stretching criterion is strictly applicable only for a brush on a flat surface. A somewhat more realistic model, in the spirit of one developed by Daoud and Cotton,[30] would be to consider each PS ligand as a sphere of radius R_g in order to compute a transition areal chain density that corresponds to

close packing of such spheres on a curved gold surface. This simple calculation yields a transition areal chain density Σ_{trans}

$$\Sigma_{trans} = \frac{1}{\pi}\left(\frac{R + R_g}{R_g R}\right)^2$$

which for a gold particle radius $R = 1.3$ nm and PS ligand $R_g = 1.56$ nm corresponds to $\Sigma_{trans} = 0.63$ chains/nm^2, closer to but still below the observed value of ∼1.4 chains/nm^2. More sophisticated self-consistent mean-field simulations will undoubtedly result in an improved estimate as will models that take into account the possibility that the thiols on the surface have lateral mobility. Nevertheless, the fact that PS ligand chains that are only slightly stretched seem to shield effectively the gold surface is reassuring. It implies that "grafting to" methods of assembling polymer ligands on nanoparticles can be effective in shielding the nanoparticle surface, even though such methods are incapable of producing highly stretched polymer brushes as surface layers.

Conclusion

In summary, we have demonstrated that the location of gold nanoparticles within a PS-*b*-P2VP matrix can be controlled simply by varying the grafting density of a polystyrene chain on the nanoparticle surface. Nanoparticles completely shielded by PS chains segregate toward the center of the PS domain. In contrast, nanoparticles partially shielded by PS ligands adsorb at the interfaces between the PS and P2VP blocks. This transition occurred as the areal chain density is decreased from 1.6 to 1.2 chains/nm^2. No such transition is observed for P2VP ligands on gold nanoparticles, demonstrating that it is the preferential interaction between the P2VP block and the imperfectly shielded Au surface that is responsible for the segregation of Au particles imperfectly shielded by PS ligands to the PS/P2VP interface. The strategy of controlling the location of nanoparticles by changing the areal density of single polymeric ligand is a simple and versatile method that can be extended to other inorganic−polymer hybrid materials.

References and Notes

(1) Bockstaller, M. R.; Lapetnikov, Y.; Margel, S.; Thomas, E. L. *J. Am. Chem. Soc.* **2003**, *125*, 5276−5277.
(2) Bockstaller, M. R.; Mickiewicz, R. A.; Thomas, E. L. *Adv. Mater.* **2005**, *17*, 1331−1349.
(3) Chiu, J. J.; Kim, B. J.; Kramer, E. J.; Pine, D. J. *J. Am. Chem. Soc.* **2005**, *127*, 5036−5037.
(4) Boontongkong, Y.; Cohen, R. E. *Macromolecules* **2002**, *35*, 3647−3652.
(5) Kim, B. J.; Chiu, J. J.; Yi, G. R.; Pine, D. J.; Kramer, E. J. *Adv. Mater.* **2005**, *17*, 2618−2622.
(6) Kane, R. S.; Cohen, R. E.; Silbey, R. *Chem. Mater.* **1999**, *11*, 90−93.
(7) Lin, Y.; Boker, A.; He, J. B.; Sill, K.; Xiang, H. Q.; Abetz, C.; Li, X. F.; Wang, J.; Emrick, T.; Long, S.; Wang, Q.; Balazs, A.; Russell, T. P. *Nature (London)* **2005**, *434*, 55−59.
(8) Misner, M. J.; Skaff, H.; Emrick, T.; Russell, T. P. *Adv. Mater.* **2003**, *15*, 221−224.
(9) Sankaran, V.; Yue, J.; Cohen, R. E.; Schrock, R. R.; Silbey, R. J. *Chem. Mater.* **1993**, *5*, 1133−1142.
(10) Spatz, J.; Mossmer, S.; Moller, M.; Kocher, M.; Neher, D.; Wegner, G. *Adv. Mater.* **1998**, *10*, 473−475.
(11) Lopes, W. A.; Jaeger, H. M. *Nature (London)* **2001**, *414*, 735−738.
(12) Tsutsumi, K.; Funaki, Y.; Hirokawa, Y.; Hashimoto, T. *Langmuir* **1999**, *15*, 5200−5203.

(13) Bronstein, L. H.; Sidorov, S. N.; Valetsky, P. M.; Hartmann, J.; Colfen, H.; Antonietti, M. *Langmuir* **1999**, *15*, 6256−6262.

(14) Sohn, B. H.; Seo, B. H. *Chem. Mater.* **2001**, *13*, 1752−1757.

(15) Thompson, R. B.; Ginzburg, V. V.; Matsen, M. W.; Balazs, A. C. *Science* **2001**, *292*, 2469−2472.

(16) Thompson, R. B.; Ginzburg, V. V.; Matsen, M. W.; Balazs, A. C. *Macromolecules* **2002**, *35*, 1060−1071.

(17) Lee, J. Y.; Thompson, R. B.; Jasnow, D.; Balazs, A. C. *Faraday Discuss.* **2003**, *123*, 121−131.

(18) Templeton, A. C.; Wuelfing, M. P.; Murray, R. W. *Acc. Chem. Res.* **2000**, *33*, 27−36.

(19) Corbierre, M. K.; Cameron, N. S.; Lennox, R. B. *Langmuir* **2004**, *20*, 2867−2873.

(20) Krausch, G. *Mater. Sci. Eng. R* **1995**, *14*, 1−94.

(21) Brust, M.; Walker, M.; Bethell, D.; Schiffrin, D. J.; Whyman, R. *J. Chem. Soc., Chem. Commun.* **1994**, 801−802.

(22) Yee, C. K.; Jordan, R.; Ulman, A.; White, H.; King, A.; Rafailovich, M.; Sokolov, J. *Langmuir* **1999**, *15*, 3486−3491.

(23) Shimmin, R. G.; Schoch, A. B.; Braun, P. V. *Langmuir* **2004**, *20*, 5613−5620.

(24) Leff, D. V.; Ohara, P. C.; Heath, J. R.; Gelbart, W. M. *J. Phys. Chem.* **1995**, *99*, 7036−7041.

(25) Hostetler, M. J.; Wingate, J. E.; Zhong, C. J.; Harris, J. E.; Vachet, R. W.; Clark, M. R.; Londono, J. D.; Green, S. J.; Stokes, J. J.; Wignall, G. D.; Glish, G. L.; Porter, M. D.; Evans, N. D.; Murray, R. W. *Langmuir* **1998**, *14*, 17−30.

(26) Kunz, M. S.; Shull, K. R.; Kellock, A. J. *J. Colloid Interface Sci.* **1993**, *156*, 240−249.

(27) Gittins, D. I.; Caruso, F. *Angew. Chem., Int. Ed.* **2001**, *40*, 3001−3004.

(28) Gandubert, V. J.; Lennox, R. B. *Langmuir* **2005**, *21*, 6532−6539.

(29) Pieranski, P. *Phys. Rev. Lett.* **1980**, *45*, 569−572.

(30) Daoud, M.; Cotton, J. P. *J. Phys. (Paris)* **1982**, *43*, 531−538.